Supporting Information

Reprogrammable Shape Memory Ion Gels via Physical Entanglement of Ultrahigh Molecular Weight Polymers

Ryota Tamate, Koichiro Uto,* Yuji Kamiyama, and Takeshi Ueki*

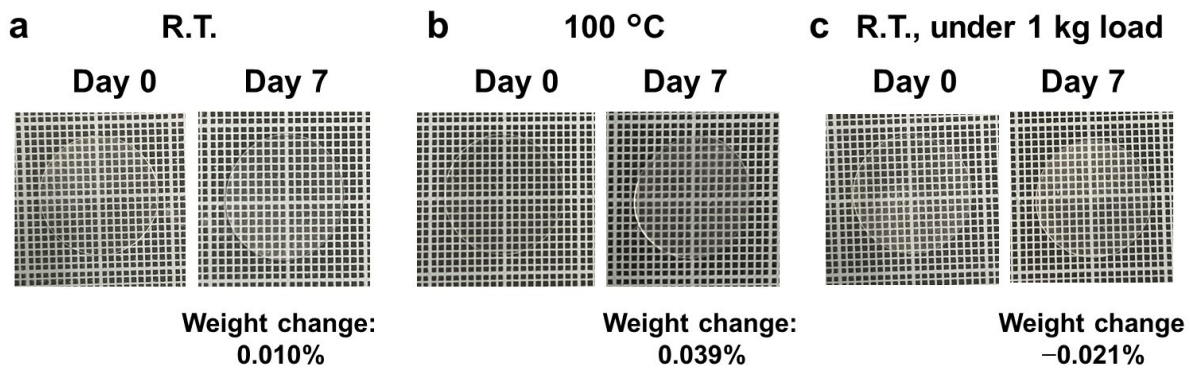

Figure S1. Appearance and mass change of disk-shaped 45 wt-PMMA-H-[C_2mim][NFSI] ion gels after one week: (a) at room temperature, (b) at elevated temperature (100 °C), and (c) under compression with a 1 kg load at room temperature. Each sample was gently wiped every 24 h, and its mass was recorded to verify the absence of ionic liquid leakage.

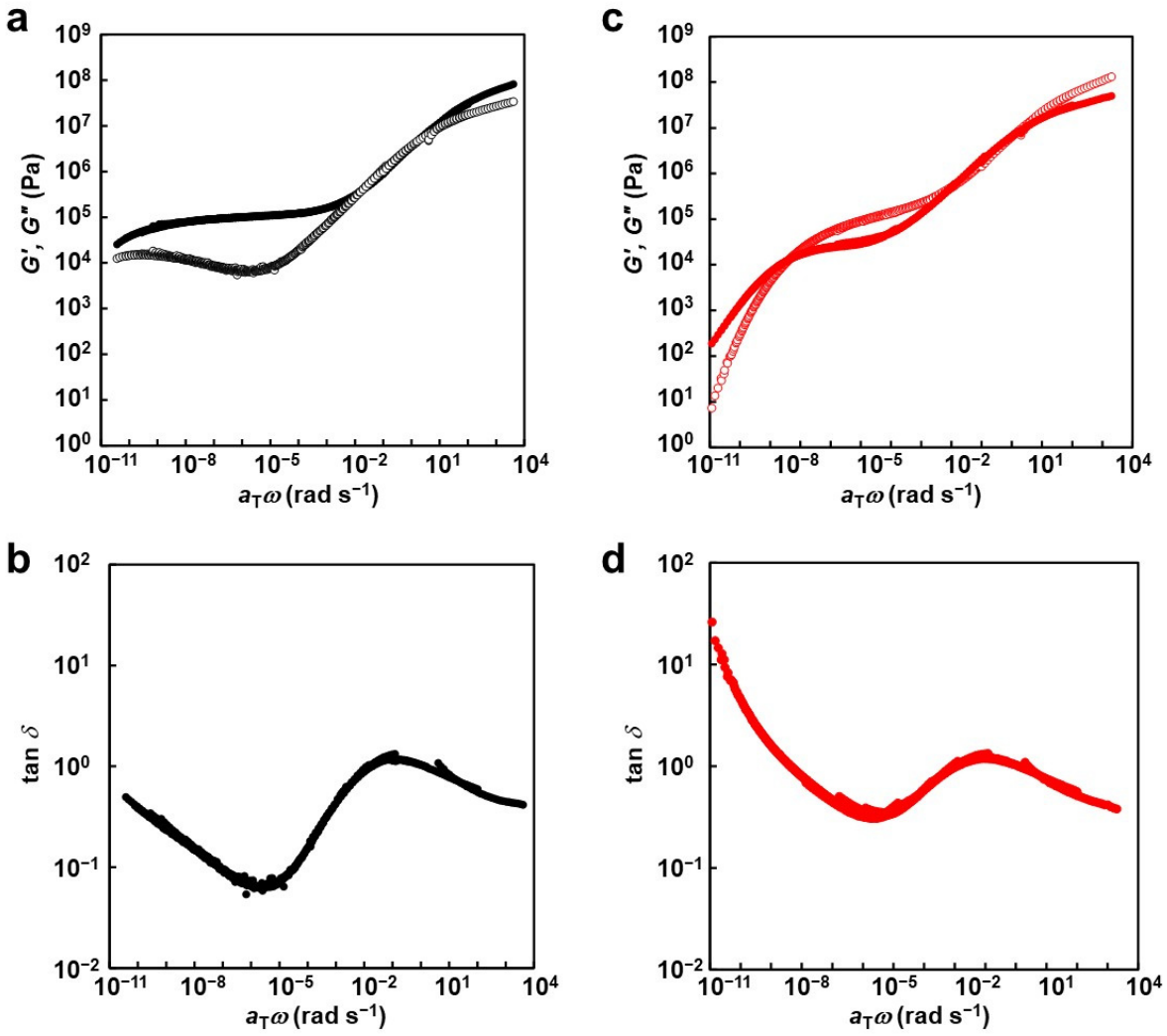

Figure S2. Viscoelastic master curves of (a, c) the storage (G') and loss (G'') moduli and (b, d) tan δ for (a, b) 45wt-PMMA-H-[C2mim][NFSI] and (c, d) 45wt-PMMA-M-[C2mim][NFSI], respectively. The reference temperature is 50 °C.

Table S1. Glass-transition temperatures (T_g) and glass-transition widths (ΔT_g) determined by DSC and rheology for the 45 wt-PMMA-H-[C2mim][NFSI] ion gel studied in this work, neat PMMA, and a commercial polyurethane-based shape-memory polymer (SMP).

Name	$T_{g,DSC}$[a]	$\Delta T_{g,DSC}$[a]	$T_{g,rheol}$[b]	$\Delta T_{g,rheol}$[b]
45wt-PMMA-H-[C2mim][NFSI]	47	34	51	36
PMMA (M_w = 120 kg mol^{-1})	118	22	117	23
Polyurethane-based SMP	50	14	51	12

[a]Evaluated by DSC. T_g was determined as the inflection point of the 2nd heating scan (10 °C min^{-1}). ΔT_g was calculated as $T_{g,\,end} - T_{g,\,onset}$. [b]Evaluated by rheological temperature sweep measurements. T_g was determined as the peak temperature of tan δ. ΔT_g was defined as the full width at half maximum (FWHM) of the tan δ peak.

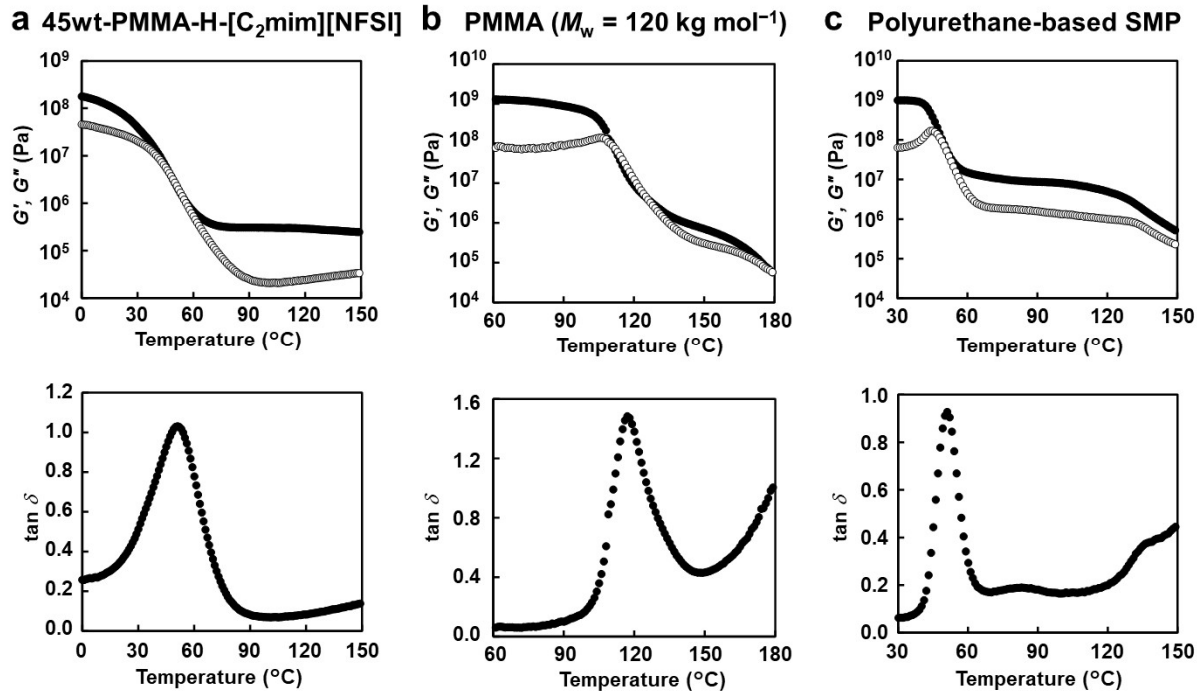

Figure S3. (a-c) Temperature dependence of the storage (G') and loss (G'') moduli (upper panels) and tan δ (lower panels) for (a) 45wt-PMMA-H-[C2mim][NFSI], (b) neat PMMA (M_w = 120 kg mol^{-1}), and (c) polyurethane-based SMP.

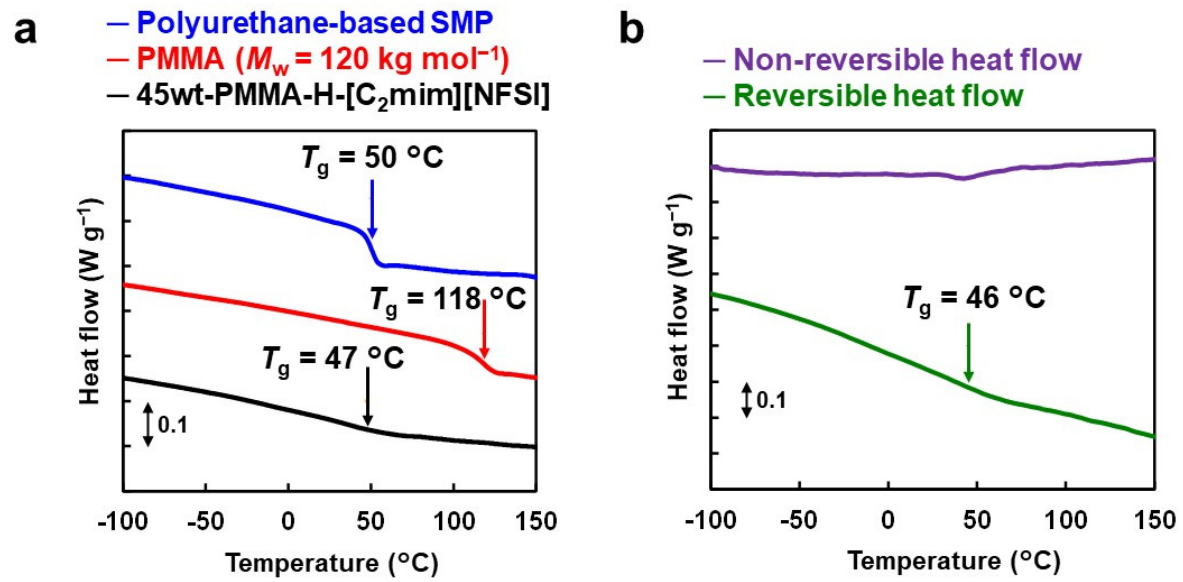

Figure S4. (a) DSC heat flow curves for 45wt-PMMA-H-[C2mim][NFSI] (black), neat PMMA (M_w = 120 kg mol^{-1}) (red), and a polyurethane-based SMP (blue). The arrows indicate the glass transition temperature (T_g) for each sample. (b) Reversible (green) and irreversible (purple) heat flow curves for 45wt-PMMA-H-[C2mim][NFSI] obtained by modulated DSC measurements. The arrow indicates the T_g obtained from the reversible heat flow curve.

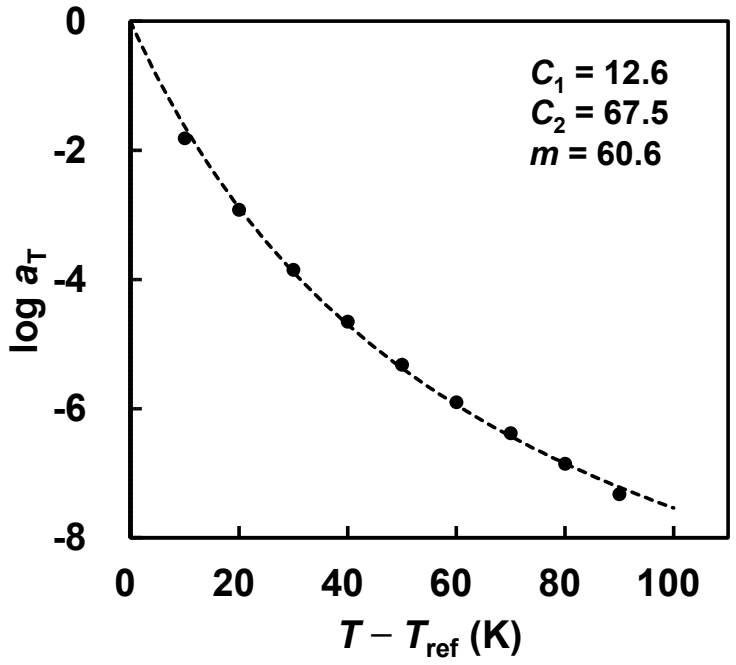

Figure S5. Temperature dependence of the horizontal shift factor a_T, obtained from the time–temperature superposition master curves of the 45wt-PMMA-H-[C2mim][NFSI] ion gel (**Figure S2**), plotted against $T-T_{ref}$, together with the fitting curve (dotted line) based on the Williams–Landel–Ferry (WLF) equation:[S1]

$$\log a_T = \frac{-C_1(T - T_{\mathrm{ref}})}{C_2 + (T - T_{\mathrm{ref}})} \quad (1)$$

where T_{ref} is the reference temperature, and C_1 and C_2 are empirical constants. The fragility index, m, was calculated according to:[S2]

$$m = \frac{C_1}{C_2} T_{\mathrm{g}} \quad (2)$$

where T_g is the glass transition temperature determined from the tan δ peak in the rheological temperature-sweep measurement (**Figure 2b**). Equation (2) can be applied when the $T_{ref} = T_g$. Because the T_{ref} used for the master curve (50 °C) was nearly identical to the rheological T_g (51 °C), the fitted parameters obtained at T_{ref} were used to estimate m. The values of the fitted WLF parameters (C_1 and C_2) and the resulting fragility index (m) are indicated in the figure.

[S1] *J. Am. Chem. Soc.*, 1955, **77**, 3701–3707.
[S2] *Polymer*, 2008, **49**, 4427–4432.

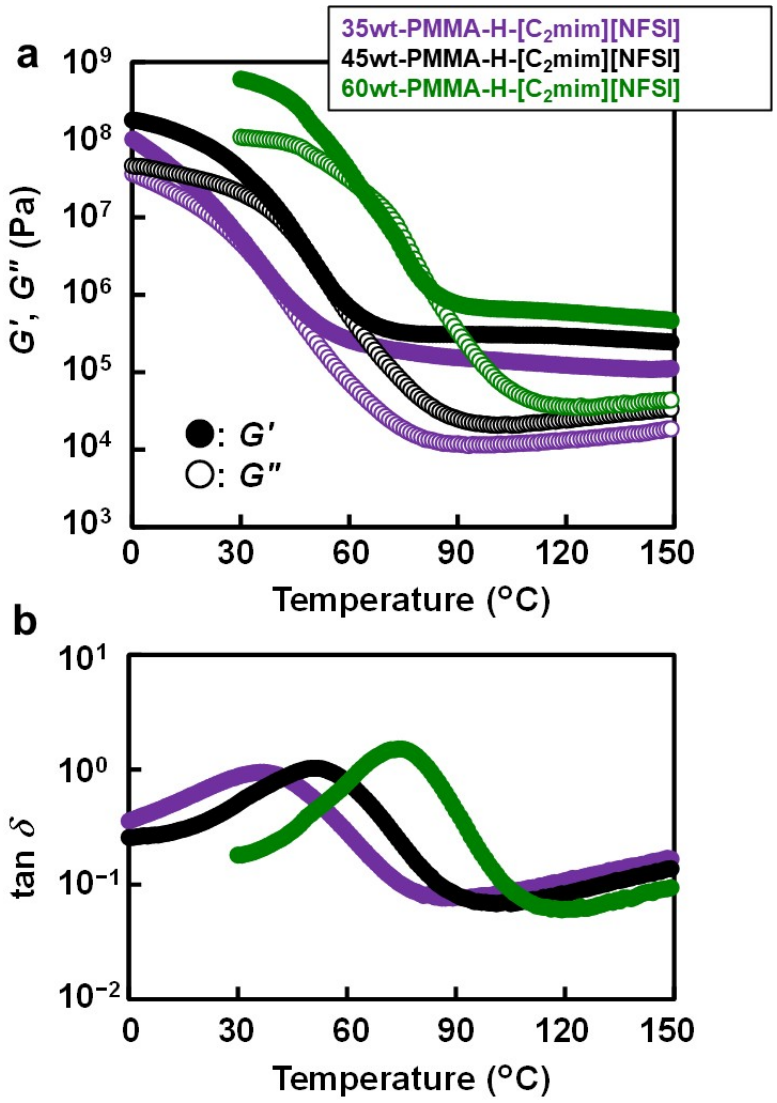

Figure S6. Temperature sweep measurements of the UHMW PMMA/[C2mim][NFSI] ion gels with different polymer concentrations showing (a) G' and G'' and (b) tan δ.

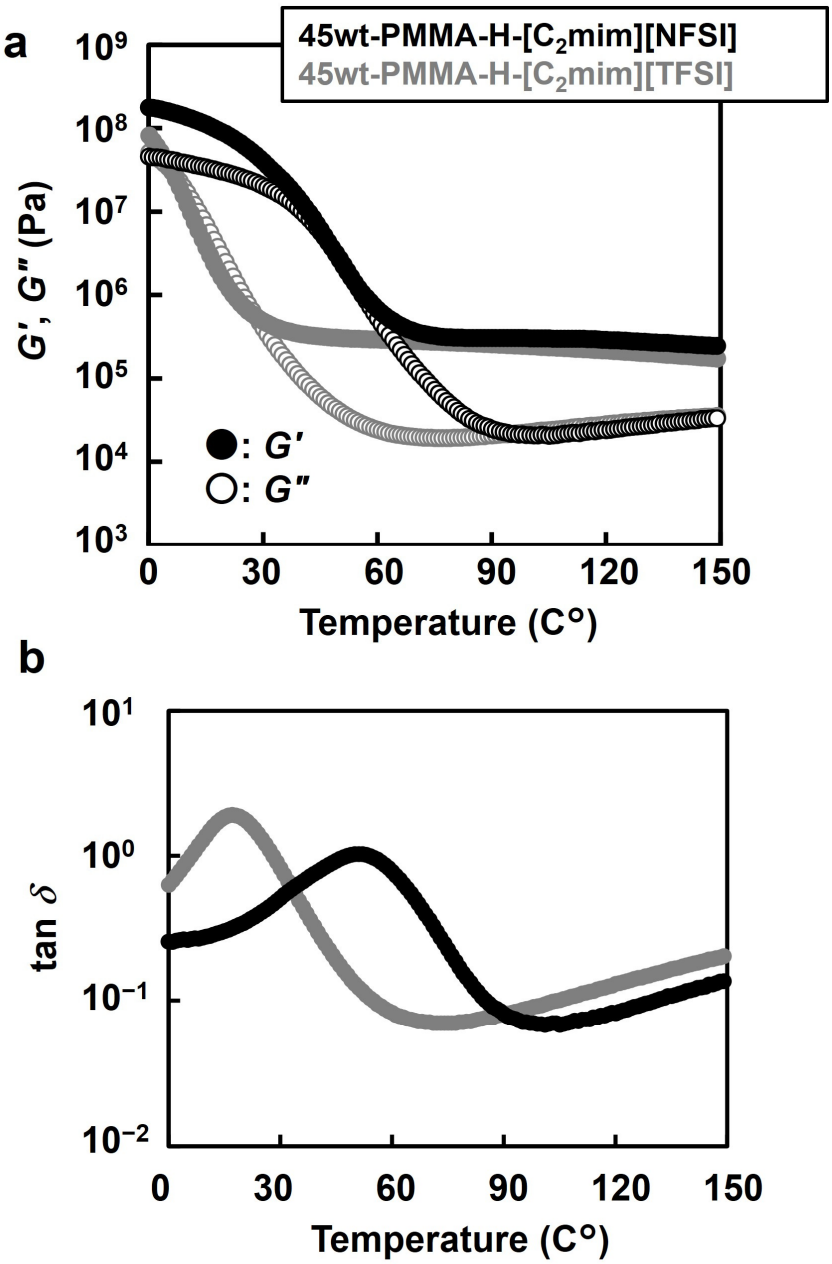

Figure S7. Temperature sweep measurements of the UHMW PMMA/IL ion gels containing TFSI and NFSI anions. (a) Storage modulus (G') and loss modulus (G''). (b) Loss tangent (tan δ).

Table S2. Tensile strength at break (σ_b), elongation at break (ε_b), and toughness of each ion gel. Values are reported as the mean ± standard deviation for $N = 3$ samples.

Name	σ_b (MPa)	ε_b (%)	Toughness (MJ m^{-3})
45wt-PMMA-H-[C_2mim][NFSI]	22.7 ± 0.8	213 ± 4	29.1 ± 1.2
45wt-PMMA-M-[C_2mim][NFSI]	19.3 ± 0.4	224 ± 3	28.6 ± 0.6
45wt-PMMA-L-[C_2mim][NFSI]	7.4 ± 0.1	93 ± 14	6.5 ± 1.0

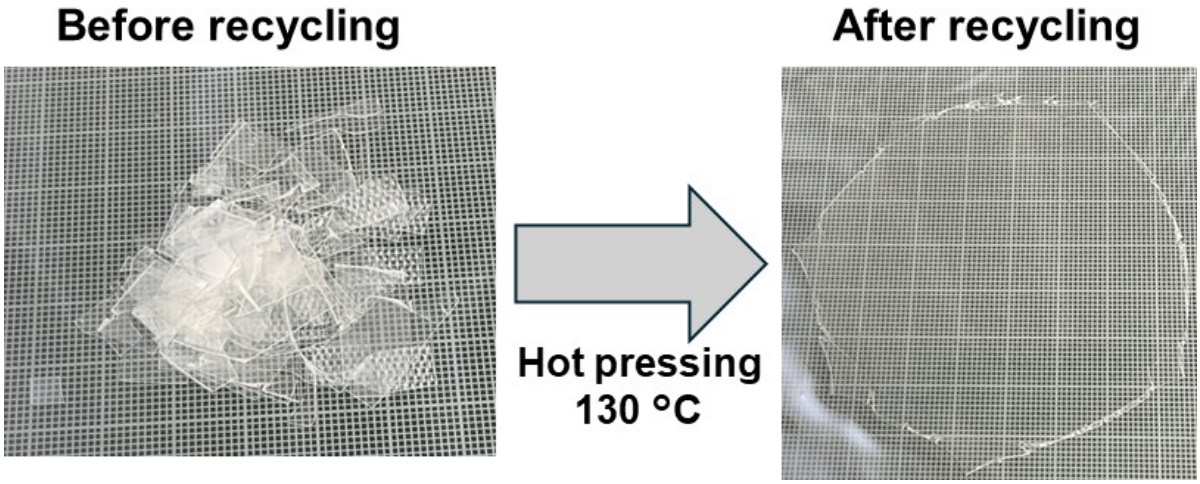

Figure S8. Photographs of the 45wt-PMMA-H-[C_2mim][NFSI] ion gel cut into small fragments prior to recycling (left) and the recycled ion gel sheet obtained after hot pressing (right).

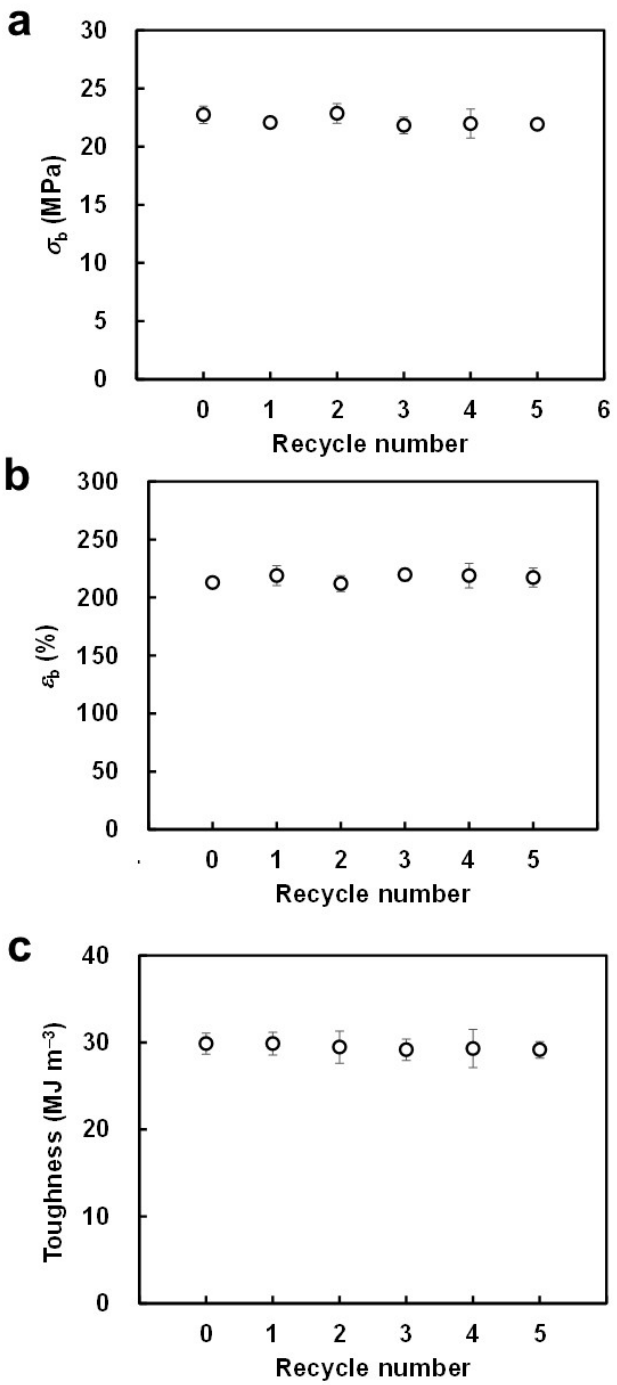

Figure S9. Changes in fracture stress (σ_b), elongation at break (ε_b), and toughness as a function of the number of recycling cycles. Cycle 0 represents the pristine sample. Error bars indicate the standard deviation of three independent samples ($N = 3$).

Table S3. Tensile strength at break (σ_b), elongation at break (ε_b), and toughness of the 45 wt-PMMA-H-[C_2mim][NFSI] ion gel in the pristine state and after each recycling cycle. Values are reported as the mean ± standard deviation for $N = 3$ samples.

Recycle number	σ_b (MPa)	ε_b (%)	Toughness (MJ m^{-3})
Pristine	22.7 ± 0.8	213 ± 4	29.1 ± 1.2
1st recycle	22.1 ± 0.5	219 ± 9	29.9 ± 1.3
2nd recycle	22.8 ± 0.8	212 ± 7	29.5 ± 1.9
3rd recycle	21.8 ± 0.7	220 ± 5	29.2 ± 1.2
4th recycle	22.0 ± 1.2	219 ± 11	29.3 ± 2.2
5th recycle	21.9 ± 0.4	217 ± 8	29.2 ± 1.0

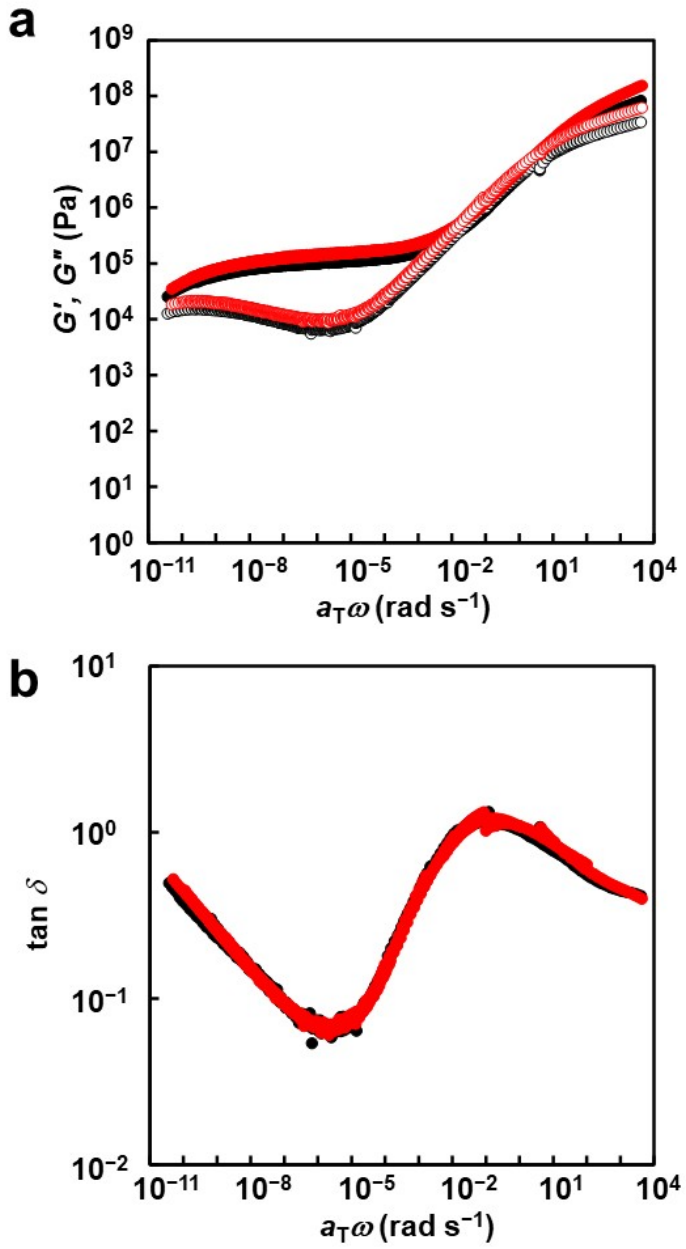

Figure S10. Viscoelastic master curves of (a) the storage (G') and loss (G'') moduli and (b) tan δ for pristine (black) and recycled (red) 45wt-PMMA-H-[C_2mim][NFSI] ion gels. The reference temperature is 50 °C.

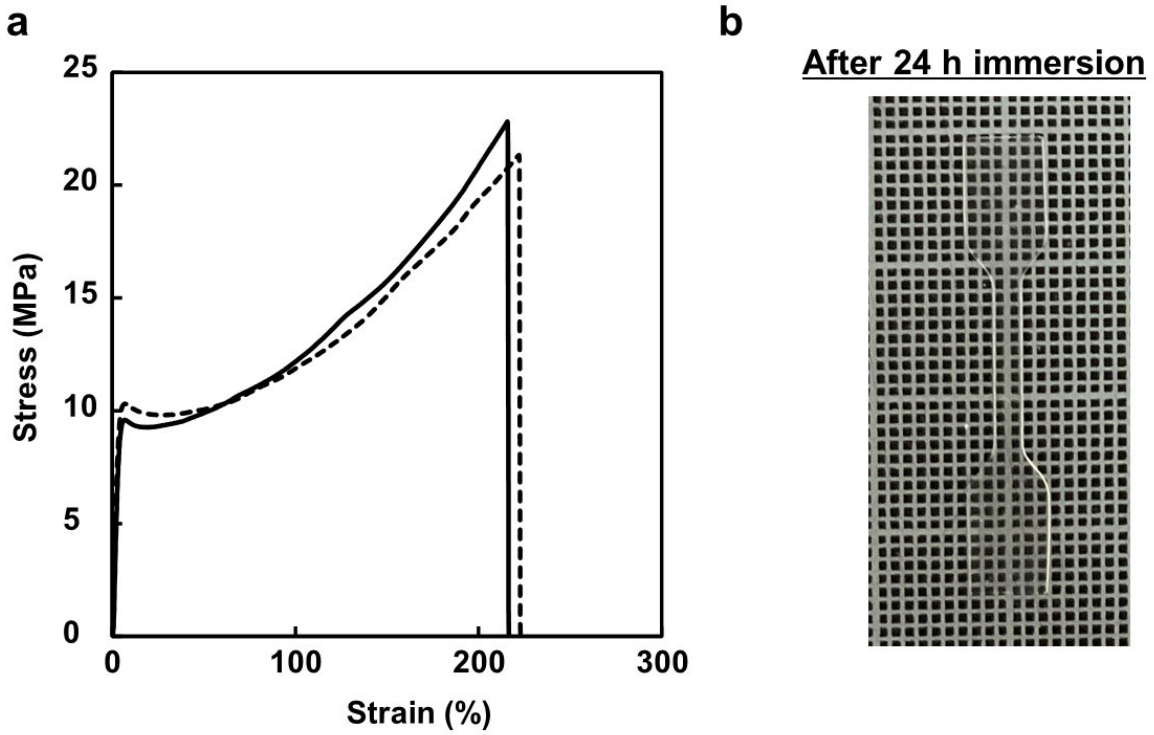

Figure S11. (a) Stress–strain curves of 45wt-PMMA-H-[C_2mim][NFSI] in the pristine state (solid line) and after immersion in water for 24 h (dotted line). (b) Photograph of the dumbbell-shaped sample after 24 h of immersion.

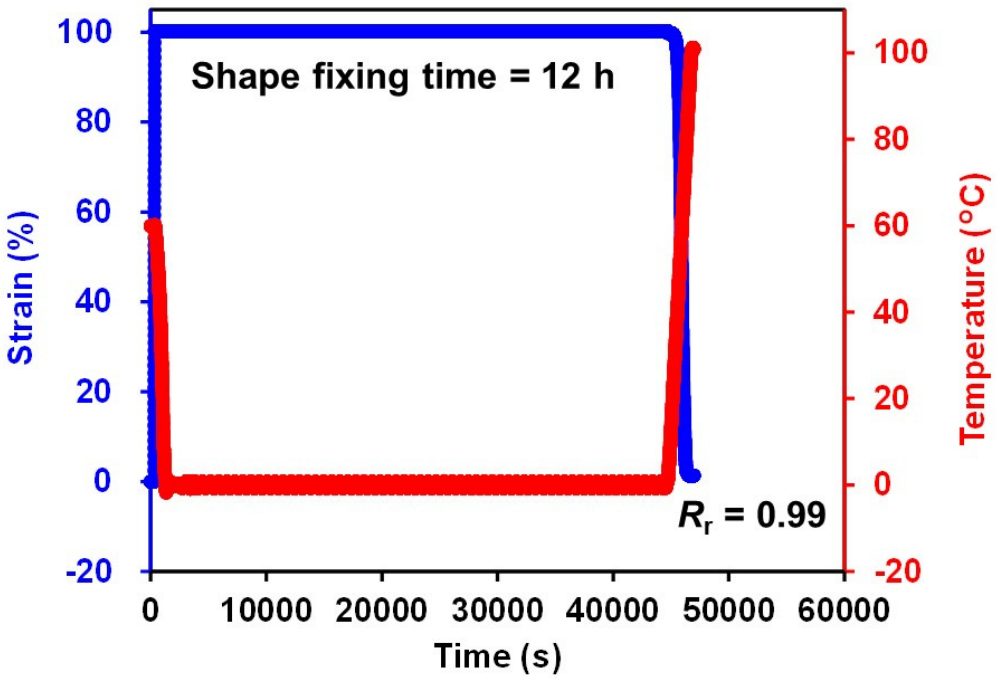

Figure S12. Shape-memory tests of 45wt-PMMA-H-[C_2mim][NFSI] measured by DMA with prolonged shape fixing process (process 2) to 12 h.

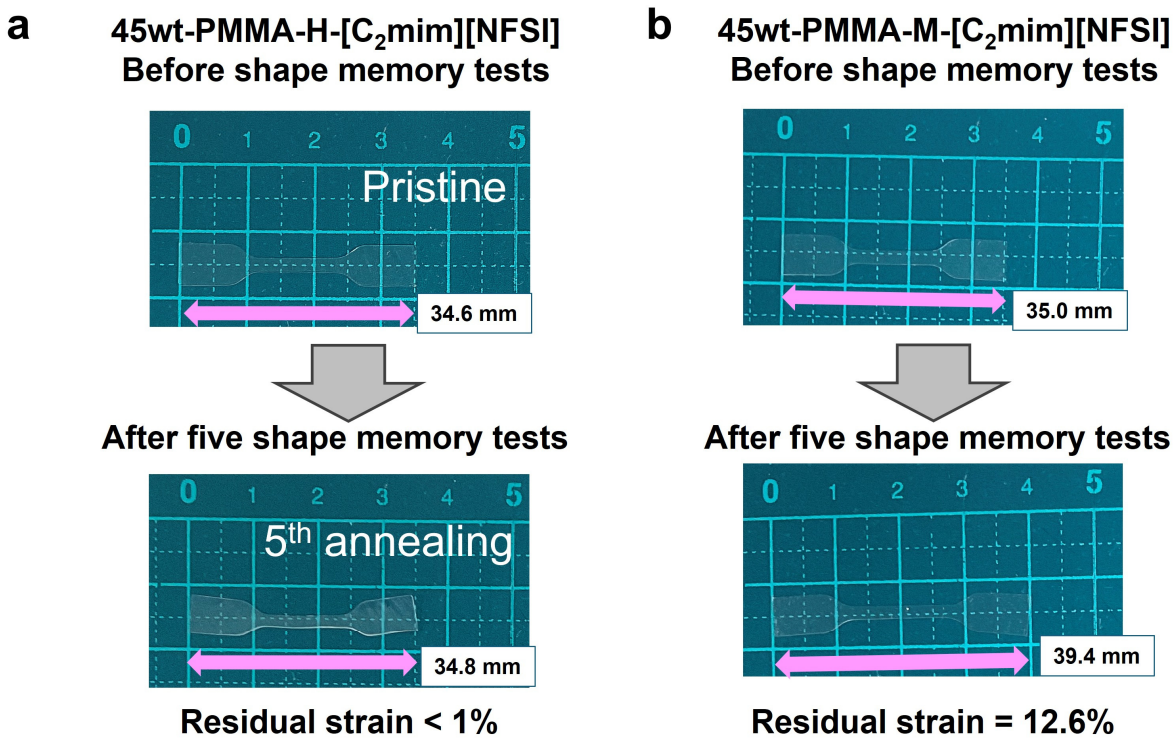

Figure S13. Changes in sample shape before and after the repeated shape memory test presented in **Figure 4c** for (a) 45wt-PMMA-H-[C_2mim][NFSI] and (b) 45wt-PMMA-M-[C_2mim][NFSI].

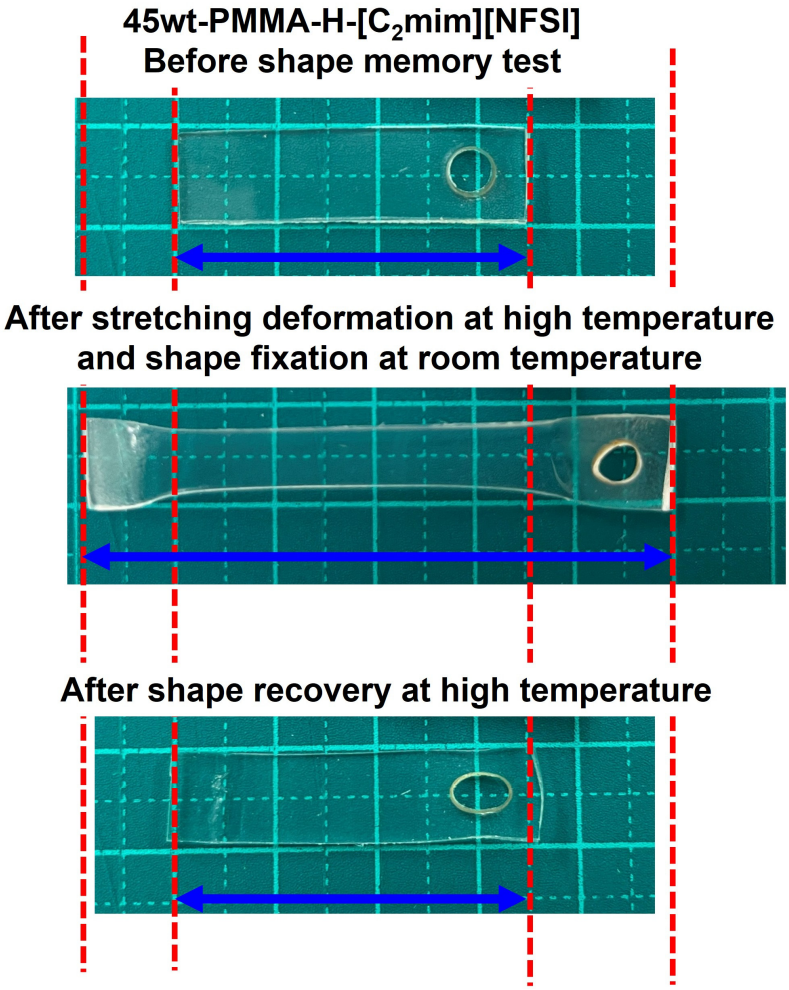

Figure S14. Photographs of the 45wt-PMMA-H-[C2mim][NFSI] ion gels before and after actuation demonstration via the shape memory process.

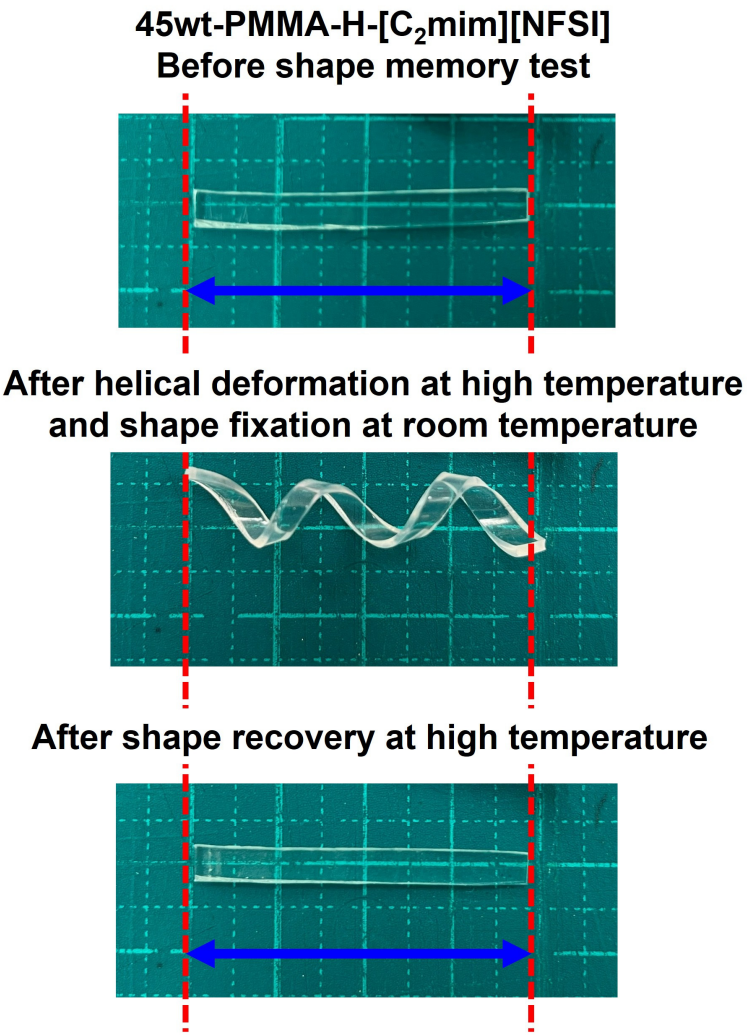

Figure S15. Photographs of the 45wt-PMMA-H-[C_2mim][NFSI] ion gel before and after shape transformation into a helical form and subsequent shape recovery.

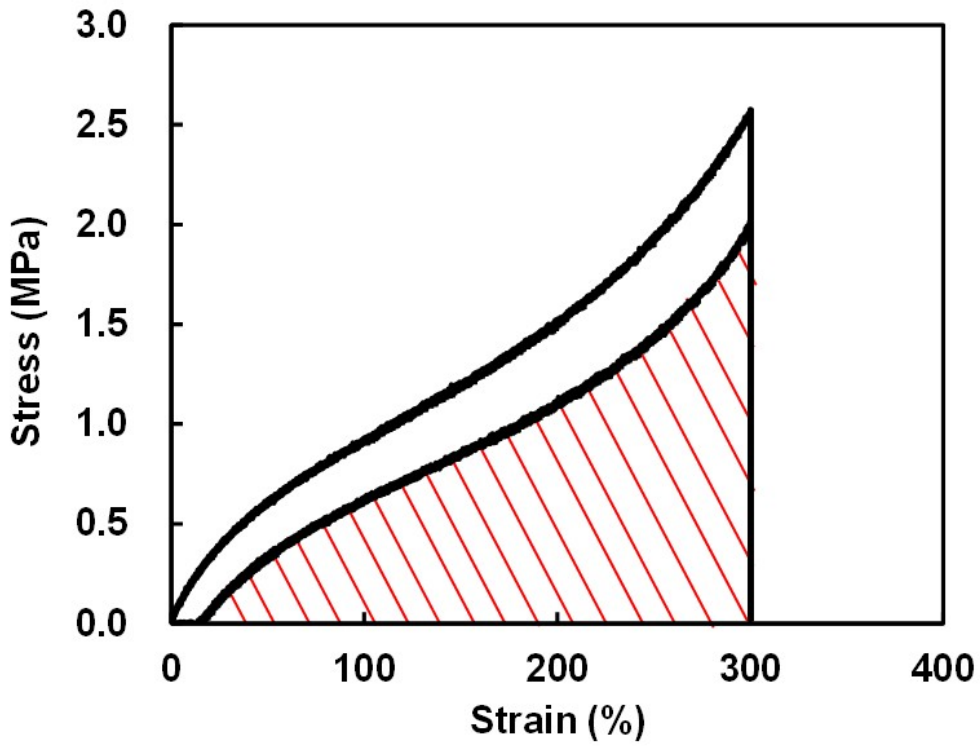

Figure S16. Loading–unloading tensile test at 80 °C up to 300% strain for evaluating the work density. The sample was stretched to 300% at a crosshead speed of 10 mm min^{-1} in a temperature-controlled chamber maintained at 80 °C (loading process), and then cooled to room temperature for 20 min to fix the temporary shape. The specimen was subsequently reheated to 80 °C, equilibrated for 10 min, and returned to the original shape at 10 mm min^{-1} (unloading process). The work density was defined as the released mechanical energy, calculated by integrating the area under the stress–strain curve during the unloading process (red hatched area).

Table S4. Comparison of the work density of previously reported shape-memory polymers/gels with that of the present study.

Sample Name	Classification	Work density ($kJ\ m^{-3}$)	Reference
90D400-10LP	Epoxy polymer	750	S3
Elastic-driven hydrogels	Hydrogel	15.3	S4
PUPCLPEG	Elastomer	717.8	S5
PAA/$Ca(CH_3COO)_2$ hydrogel	Hydrogel	45.2	S6
TCLCG	Organogel	105	S7
O_4M_1 eutectogel	Eutectogel	21	S8
Water-shrink (WS) films	Polymer film	1,028	S9
PAA ionogels	Ion gel	238	S10
Magnetic SMP	Polymer composite	1,370	S11
45wt-PMMA-H-[C_2mim][NFSI]	Ion gel	2,629	This work

[S3] *J. Polym. Sci., Part B: Polym. Phys.* **2016,** *54*, 1002–1013.

[S4] *Sci. Adv.* **2020,** *6*, eabd2520

[S5] *J. Mater. Chem. B* **2021,** *9*, 7371–7380.

[S6] *Sci China Mater* **2022,** *65*, 2274-2280.

[S7] *Adv. Mater.* **2023,** *35,* 2210419.

[S8] *ACS Appl. Mater. Interfaces* **2024,** *16*, 6424-6432

[S9] *Adv. Mater.* **2024**, *36*, 2403551

[S10] *CCS Chem.* **2025,** *7*, 2086–2097

[S11] *Adv. Funct. Mater.* **2026**, *36*, e16218

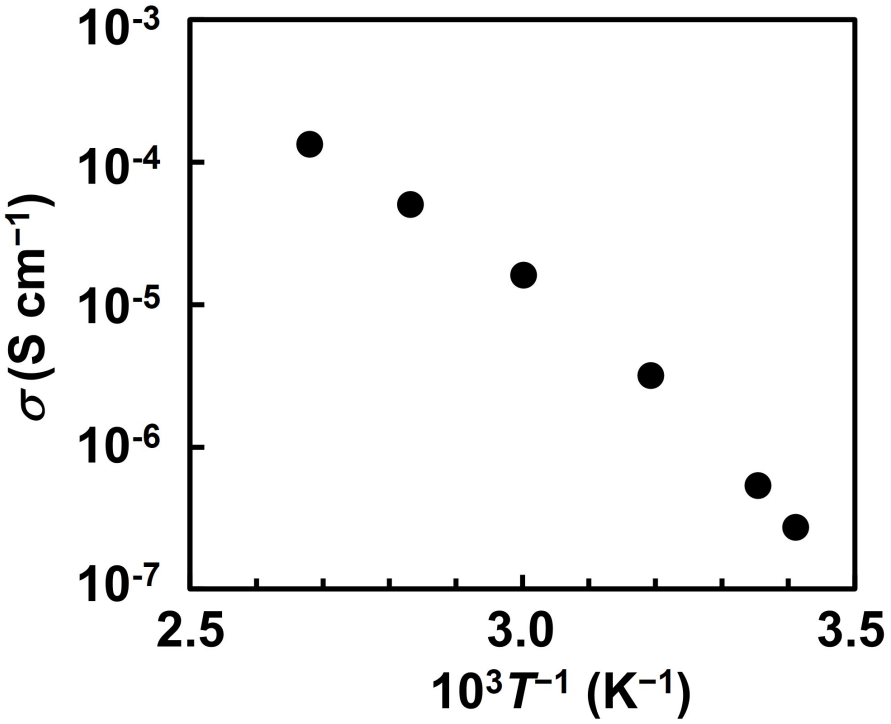

Figure S17. Temperature dependence of the ionic conductivity for the 45wt-PMMA-H-[C_2mim][NFSI] ion gel.

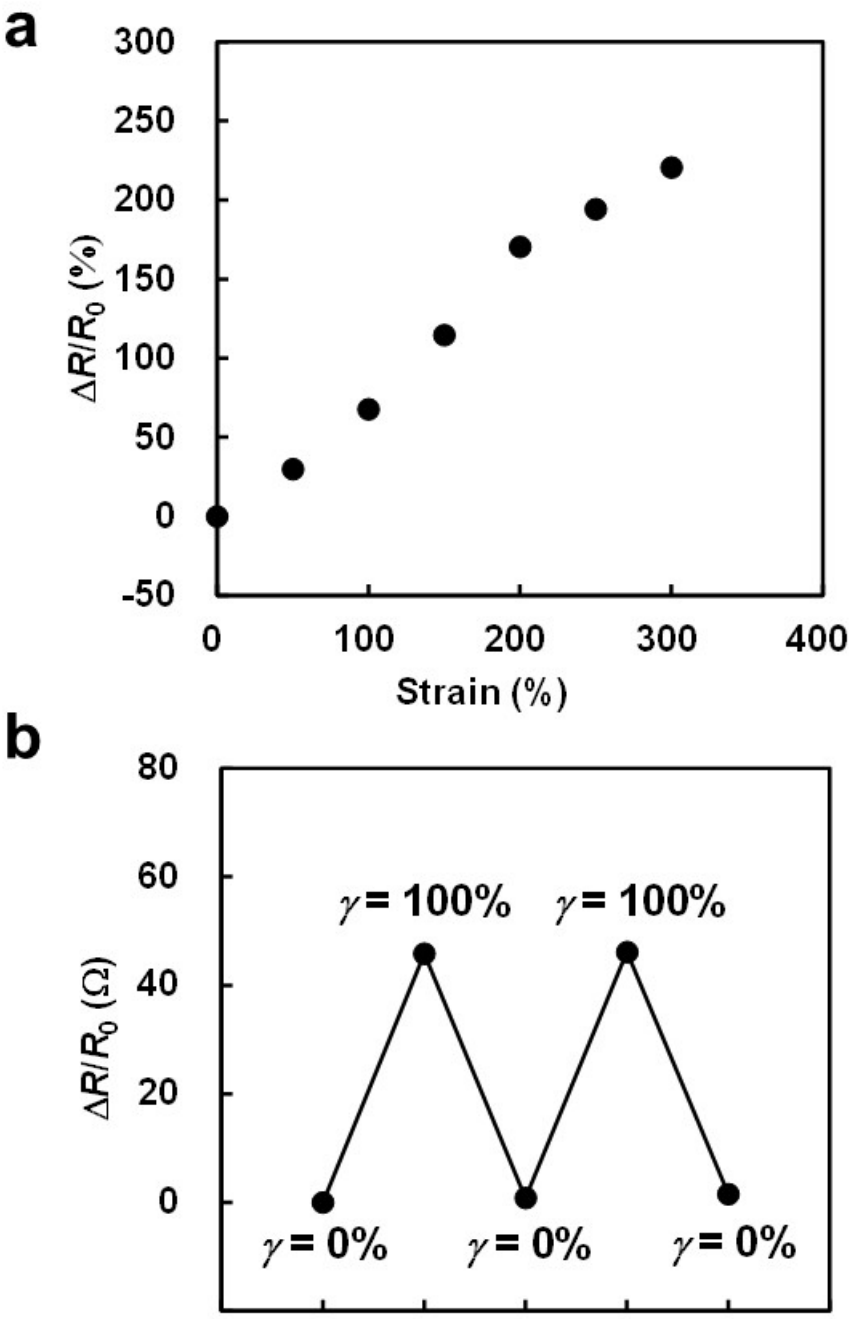

Figure S18. (a) Change in the relative resistance ($\Delta R/R_0$) of the 45 wt-PMMA-H-[C_2mim][NFSI] ion gel at 80 °C during tensile deformation. (b) Change in the relative resistance during repeated stretching to 100% strain and subsequent shape recovery at 80 °C.

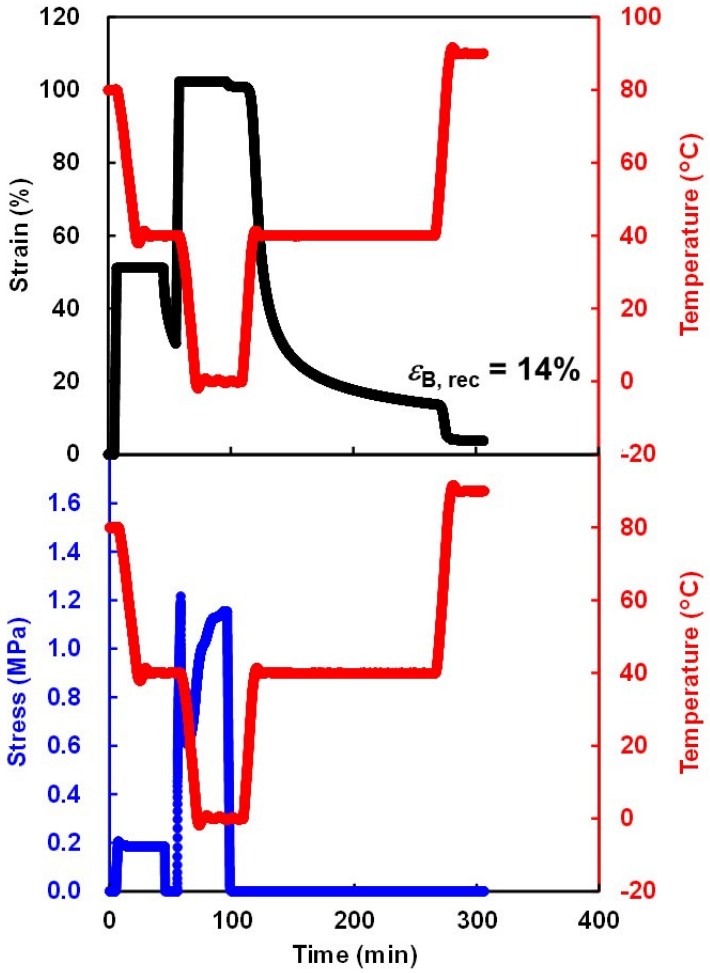

Figure S19. TSCP evaluated by DMA for the 45 wt-PMMA-H-[C_2mim][NFSI] ion gel with the recovery time for Shape B extended to 150 min. The upper panel shows the temperature and strain profiles during TSCP, whereas the lower panel shows the temperature and stress profiles.

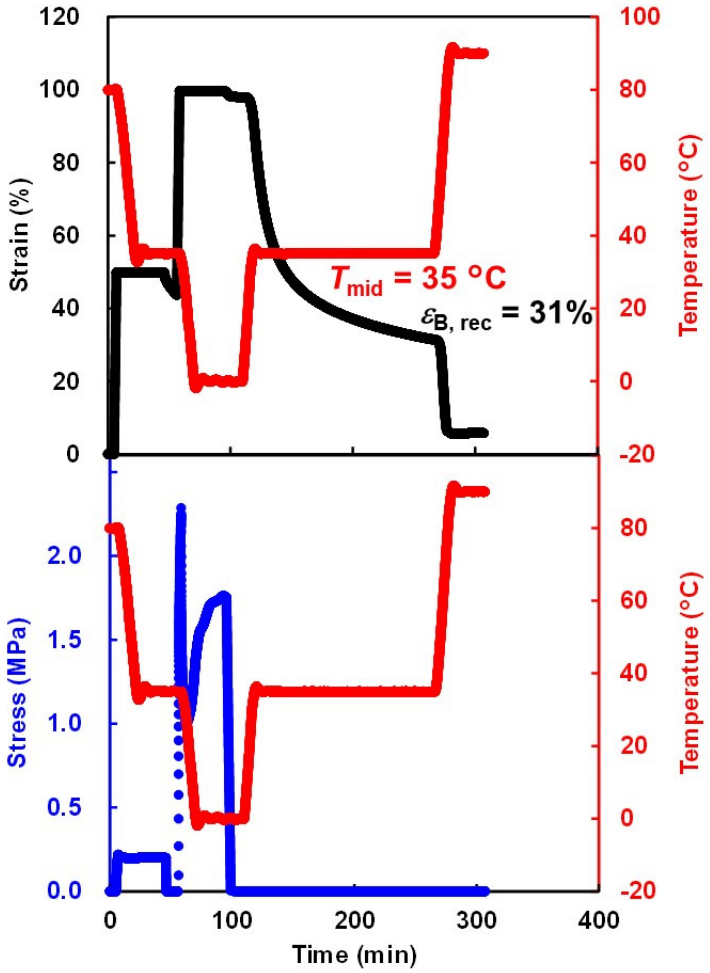

Figure S20. TSCP evaluated by DMA for the 45 wt-PMMA-H-[C2mim][NFSI] ion gel with the recovery time for Shape B extended to 150 min. Compared with Figure S18, T_{mid} was lowered from 40 to 35 °C. The upper panel shows the temperature and strain profiles during TSCP, whereas the lower panel shows the temperature and stress profiles.

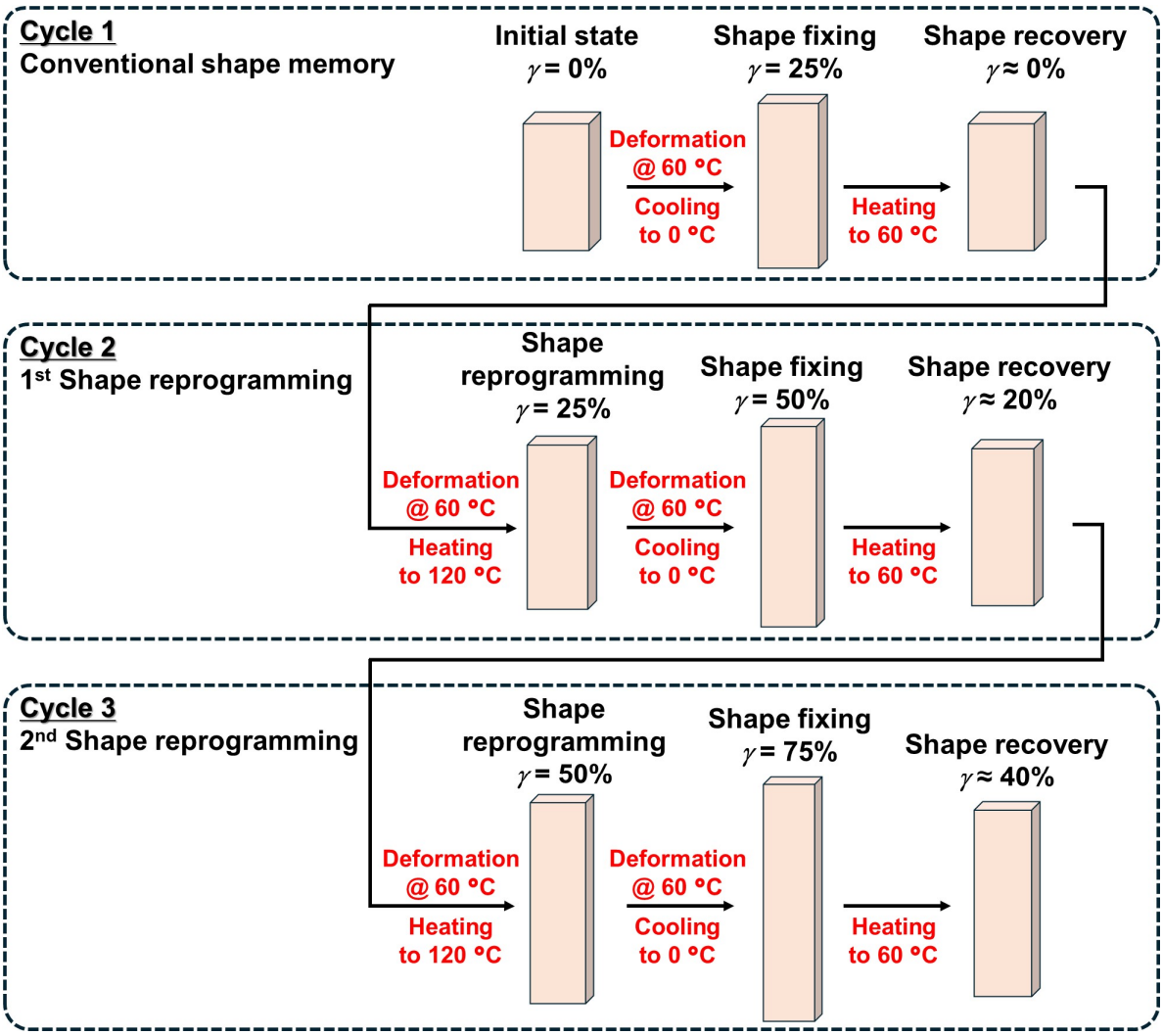

Figure S21. Schematic illustration of the deformation sequence in each cycle of the DMA-based shape-reprogramming test in Figure 6.

Movie S1. Actuation demonstration of a 45wt-PMMA-H-[C_2mim][NFSI] sheet. A rectangular sheet (0.62 g) was stretched to ~170% strain at a high temperature (> T_g) followed by cooling to room temperature to fix the deformed shape. Upon heating at 100 °C in an oven with a 100-g weight suspended, the sheet recovered its original shape, lifting the weight and demonstrating its actuation capability. The movie is played at 10× speed.

Movie S2. Shape transformation demonstration of a helical-shaped 45wt-PMMA-H-[C_2mim][NFSI] sheet. The deformed helical sample was placed in an oven at 100 °C, where it gradually unfolded and returned to its original straight sheet form. The movie is played at 10× speed.

Movie S3. Demonstration of shape reprogramming. When immersed in hot water, the reprogrammed sample (right) retained its helical shape with minimal deformation, whereas the control sample (left) reverted to a flat strip configuration.

Movie S4. Shape memory test for the control and reprogrammed samples. Both samples were temporarily deformed into a rolled shape and cooled in ice water to fix the temporary configuration. Upon heating in hot water, the reprogrammed sample (right) recovered its helical shape, while the control sample (left) returned to the flat strip configuration, indicating that its high shape memory performance is maintained following permanent shape reprogramming.

Movie S5. Shape memory behavior of the control and 2nd shape-reprogrammed samples. A control sample and a 2nd reprogrammed sample were initially reprogrammed from a helical to a ring shape, followed by temporary deformation into a ring shape and cooling in ice water to fix the temporary shape. Upon heating in hot water, only the reprogrammed sample recovered its reprogrammed ring shape, confirming successful 2nd permanent reprogramming.